

Charge density in $\text{Cu}(\text{glygly})(\text{OH}_2)_2 \cdot \text{H}_2\text{O}$ at 10 K and the reproducibility of atomic orbital populations†

Ian Bytheway, Brian N. Figgis* and Alexandre N. Sobolev

Chemistry Department, University of Western Australia, Nedlands, W. A. 6009, Australia

Received 29th March 2001, Accepted 5th October 2001

First published as an Advance Article on the web 1st November 2001

An extensive accurate X-ray data set for diaqua(glycylglycinato)copper(II) hydrate, $\text{Cu}(\text{glygly})(\text{OH}_2)_2 \cdot \text{H}_2\text{O}$, at 10 K is reported. The molecular structure is very accurately defined. The $\text{Cu}(\text{glygly})(\text{OH}_2)_2$ unit approximates to a square pyramid with the apical water molecule only loosely bound. The data have been analysed by multipole and valence orbital population models and the topology of the electron density has been examined for chemical bonding features. There are two independent molecules of the complex in the unit cell, and the agreement between their bonding features is used as a measure of the validity of obtaining quantitative valence-related parameters from X-ray data. The agreement is quite reasonable. Atomic charges evaluated by the Stockholder and monopole population methods do not conform with chemical expectations. Those from the sum of valence orbital populations and the atom-in-molecules approach are more reasonable but contain anomalies. The ‘hole’ in the $3d^{10}$ shell corresponding to the $3d^9$ configuration, predicted on the grounds of ligand field theory, is seen as a much lowered (1.16 e) population of $3d_{z^2}$ relative to the other $3d$ orbitals (av. 1.65 e). Populations of valence hybrid orbitals conform with chemical expectations and, for the $(\text{sp}^2)_\sigma$ hybridised carbon atoms of $\text{C}=\text{O}$ groups, relocation of electrons from a p_π orbital to those σ hybrids is seen. Bond critical points have been located between all the appropriate non-hydrogen atom pairs. The electron densities at these points show values typical for mixed ionic/covalent character in the $\text{Cu}-\text{O}$ and $\text{Cu}-\text{N}$ interactions and of covalent character in the $\text{C}-\text{C}$, $\text{O}-\text{C}$ and $\text{N}-\text{C}$ bonds. The Laplacian of the density at the bond critical points also behaves in a fashion which conforms with those bond types, although the scatter in the results is greater. There is little evidence of the copper atom having influenced the electron densities of the bonds between light atoms within the glycylglycinato moiety.

Introduction

Polypeptide complexes of transition metal ions are of obvious interest in biological chemistry, and information about their experimental electron density distributions could have much value. Also, while experimental charge density parameters are regularly accompanied by least-squares errors, it is known that the latter are underestimates. Because of changes in chemical and crystal environments, it rarely has been possible to obtain more realistic errors by, say, examining the same chemical moiety in different charge density studies.

In this paper we present a charge density study of the simplest ‘poly’ peptide complex of bivalent copper, diaqua(glycylglycinato)copper(II) hydrate ($\text{Cu}(\text{glygly})$). The study was carried out at 10 K to maximise the deconvolution of the valence electron shape information from the atomic thermal motions. Further, it was carried out on a system containing two completely independent units of the complex with entirely similar chemical surroundings. That has allowed the agreement between the parameters defining their valence electron distribution properties to be examined.

Monohydrate,¹ dihydrate² and trihydrate³ complexes of $\text{Cu}(\text{II})$ with the ligand glycylglycine have been reported. From the usual point of view of a charge density experiment, of them the dihydrate complex, crystallising in the monoclinic cell $C2/c$ with eight symmetry-related molecules, appears to be the most

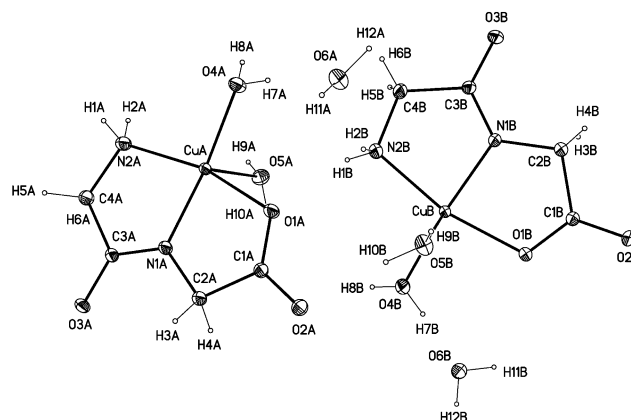


Fig. 1 The molecules in the asymmetric unit of $\text{Cu}(\text{glygly})(\text{OH}_2)_2 \cdot \text{H}_2\text{O}$ with numbering scheme.

suitable. Less attractive is the trihydrate, which also crystallises in a monoclinic cell, $P2_1/c$, but which has four molecules of each of two independent but chemically entirely similar types. The asymmetric unit consists of two $\text{Cu}(\text{glygly})(\text{H}_2\text{O})_2 \cdot \text{H}_2\text{O}$ units. We were unable to obtain the dihydrate, and proceeded to study the trihydrate. The molecule of the trihydrate, with the atom numbering scheme employed, is shown in Fig. 1 and the unit cell contents in Fig. 2.

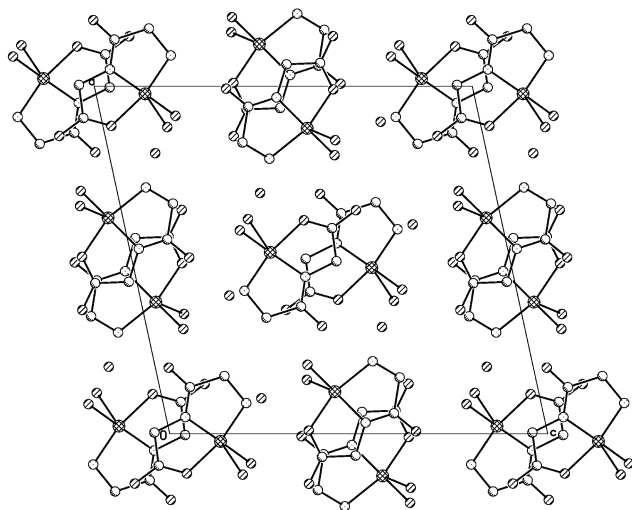
Experimental

The method set out by Kistenmacher and Szalda³ for the preparation of $\text{Cu}(\text{glygly}) \cdot 2\text{H}_2\text{O}$ was followed carefully, but

† Electronic supplementary information (ESI) available: atomic fractional cell coordinates (293 and 10 K), μ_{eq} (293 and 10 K); selected bond lengths and angles; anisotropic displacement factors (spherical, 293 and 10 K; multipole, 10 K; valence orbital, 10 K), structure factors (spherical, 293 and 10 K; multipole, 10 K). See <http://www.rsc.org/suppdata/dt/b1/b102891j/>

Table 1 Crystal and X-ray data collection details for Cu(glygly)-(OH)₂·H₂O

Temperature/K	293(2)	10(1)
Crystal size/mm	0.68 × 0.38 × 0.35	0.68 × 0.38 × 0.35
Empirical formula	C ₄ H ₁₂ CuN ₂ O ₆	C ₄ H ₁₂ CuN ₂ O ₆
Formula weight	247.70	247.70
<i>F</i> (000)	1016	1016
Crystal system	Monoclinic	Monoclinic
Space group	<i>P</i> 2 ₁ / <i>n</i>	<i>P</i> 2 ₁ / <i>n</i>
<i>Z</i>	8	8
<i>D</i> _c /g cm ⁻³	1.892	1.934
<i>μ</i> /mm ⁻¹	2.515	2.571
<i>a</i> /Å	14.962(2)	14.8413(9)
<i>b</i> /Å	7.5234(9)	7.4402(5)
<i>c</i> /Å	15.804(2)	15.765(2)
<i>β</i> /°	102.137(9)	102.242(5)
Volume/Å ³	1739.2(4)	1701.2(3)
<i>θ</i> range/°	1.7–25.0	1.7–50.1
<i>h</i> range	0→17	–32 to 29
<i>k</i> range	0→8	–15 to 15
<i>l</i> range	–18 to 18	–34 to 34
Reflections collected	3191	68042
Independent refln.	3075	17828
<i>R</i> (int)	0.0102	0.0268
Transmission (max)	0.5307	0.5234
Transmission (min)	0.4148	0.3810

**Fig. 2** Projection of the unit cell contents onto the *a*–*c* plane for Cu(glygly)(OH)₂·H₂O.

repeatedly resulted in the crystallisation of the trihydrate as well formed deep blue prisms.

An X-ray data set (*β*-filtered radiation, $\lambda(\text{Mo-K}\alpha) = 0.71073$ Å) was obtained from a crystal with maximum dimensions $0.68 \times 0.38 \times 0.35$ mm, which was mounted on a locally assembled Huber 512 goniometer⁴ equipped with a Displex 202D cryogenic refrigerator, at the Department of Chemistry of the University of Western Australia. The temperatures employed were 293(2) and 10(1) K. Data analysis was performed with the profile-fitting program PROFIT.⁵ During data reduction, intensities collected at 10 K were corrected for the absorption by the beryllium cylinder shields. Correction for the X-ray radiation absorption by the crystal was performed with XTAL^{6a} using a Gaussian integration over all the path lengths for all the grid points to give the absorption correction for each reflection. Details of the data collection are given in Table 1.

CCDC reference numbers 162657–162660 for the 293 K spherical atom and 10 K spherical atom, multipole and valence orbital refinements.

See <http://www.rsc.org/suppdata/dt/b1/b102891j/> for crystallographic data in CIF or other electronic format.

Refinements

All refinements included a correction for Type II extinction based on the model of Becker and Coppens.⁷

Spherical atom refinement

We employed the atom numbering system and initial coordinates of Kistenmacher and Szalda.³ Refinements were carried out with the SHELXL97⁸ program. Neutral atomic scattering factors were taken from ref. 9.

Models were refined, minimizing the quantity $\sum w(F_{\text{obs}}^2 - F_{\text{calc}}^2)/\sum wF_{\text{obs}}^2$, with *w* defined in Table 2. Corrections for extinction (secondary, with $F_{\text{calc}}^* = kF_{\text{calc}}(1 + 0.001\chi F_{\text{calc}}^2\lambda^3/\sin 2\theta)^{1/4}$, where χ is an extinction coefficient) were carried out. The values of *R*-factors, $R = \sum ||F_{\text{obs}}| - |F_{\text{calc}}||/\sum |F_{\text{obs}}|$, and the goodness of fit parameter $\chi = \{\sum [w(F_{\text{obs}}^2 - F_{\text{calc}}^2)^2]/(n - p)\}^{1/2}$, where *n* is the number of reflections and *p* is the number of parameters refined, are presented in Table 2. Non-hydrogen atoms were refined anisotropically and H atoms isotropically in both the room and the very low temperature data refinements. The positional and equivalent isotropic atomic displacement parameters (ADP) are listed for both temperatures in Table S1 (ESI) and selected bond lengths and angles in Table S2 (ESI). Calculated C–H bonds varied from 0.90 to 1.02 Å for the room temperature data, and from 0.93 to 0.99 Å for those at low temperature; correspondingly, N–H 0.76–0.92 and 0.83–0.89; O–H 0.68–0.94 and 0.79–0.88 Å. The anisotropic ADP of non-hydrogen atoms (Table S3a,c) and the $F_{\text{obs}}/F_{\text{calc}}$ (Table S3b,d) are available as ESI.

The highest residual electron density peak found after final refinement with low temperature data ($0.86 \text{ e } \text{\AA}^{-3}$) occurred close to the middle of the double bond C1A=O2A with the distances of 0.60 Å to C1A and 0.65 Å to atom O2A. All other strong residual electron density peaks are located at positions close to the centres of covalent bonds between non-hydrogen atoms. The deepest hole, of $1.24 \text{ e } \text{\AA}^{-3}$, is 0.49 Å from atom CuA.

Multipole refinement

The program XD^{6b} was employed to produce a conventional reciprocal space multipole analysis of the 10 K X-ray data with functions chosen to match the crystallographic site symmetries of atoms. Hydrogen atom positions were calculated using O–H, N–H and C–H bond lengths known from many neutron diffraction structural studies, *viz.* 0.99, 1.01 and 1.09 Å respectively. Multipoles to order four (hexadecapoles) were employed on the copper and carbon atoms, to order three (octapoles) on the other non-hydrogen atoms and to order unity (dipoles) on the hydrogens. Neutral atom form factors derived from Clementi and Roetti constants¹⁰ were used. Two expansion/contraction parameters (*κ*) were introduced for non-hydrogen atoms, with one pertaining to the spherical portion and another for all the aspherical functions for each type of atom. For the hydrogen atoms a single value of 1.16, which was not refined, was adopted.¹¹ Details of the refinement are given in Table 2. The positional parameters and the equivalent ADP are presented in Table S1 (ESI), bond lengths and angles in Table S2 (ESI). The anisotropic ADP, the $F_{\text{obs}}/F_{\text{calc}}$ and the XD multipole coefficients are deposited in Table S3e–g. Residual density maps are presented in the best-fit plane through the copper and glygly ligand atoms for each of molecules A and B in Fig. 3a and 3b. Maps of the Laplacian of the model density, for molecules A and B respectively, are presented in the same planes (Fig. 4a and 4b) and also in the planes containing the copper and the two oxygen atoms of water molecules bonded to it (Fig. 5a and 5b).

Valence orbital refinement

The 10 K data were also analysed using the modified multipole approach where functions corresponding to real space hybrid

Table 2 Refinements of the X-ray data for Cu(glygly)(OH)₂·H₂O

<i>T</i> /K	Model	Weighting scheme	<i>N</i> _v ^e	<i>R</i> _{2σ} ^f	<i>R</i> _w ^g	<i>χ</i> ^h
293	Sph. ^a	<i>w</i> = SHELX97 ^d	332	0.0248	0.0661	1.16
10	Sph. ^a	<i>w</i> = SHELX97 ^d	332	0.0252	0.0608	1.10
10	Multi. ^b	<i>w</i> = (σ + 0.02 <i>F</i> ² + 5.0) ⁻²	800	0.0212	0.0460	1.36
10	V.O. ^c	<i>w</i> = (σ + 0.02 <i>F</i> ² + 5.0) ⁻²	480	0.0223	0.0509	1.48

^a Spherical atom. ^b XD multipole. ^c ASRED valence orbital. ^d *w* = [σ²(*F*_{obs}²) + (*AP*)² + *BP*], where *P* = (*F*_{obs}² + 2*F*_{calc}²)/3. ^e Number of variables. ^f Reliability index, *R*_{2σ} = Σ||*F*_{obs}|| - ||*F*_{calc}||/Σ||*F*_{calc}|| for data with *F*² > 2σ(*F*²). ^g Weighted reliability index, *R*_w = {Σ[*w*(*F*_{obs}² - *F*_{calc}²)]²/Σ(*F*_{obs}²)²}^{1/2} for all data. ^h Goodness-of-fit.

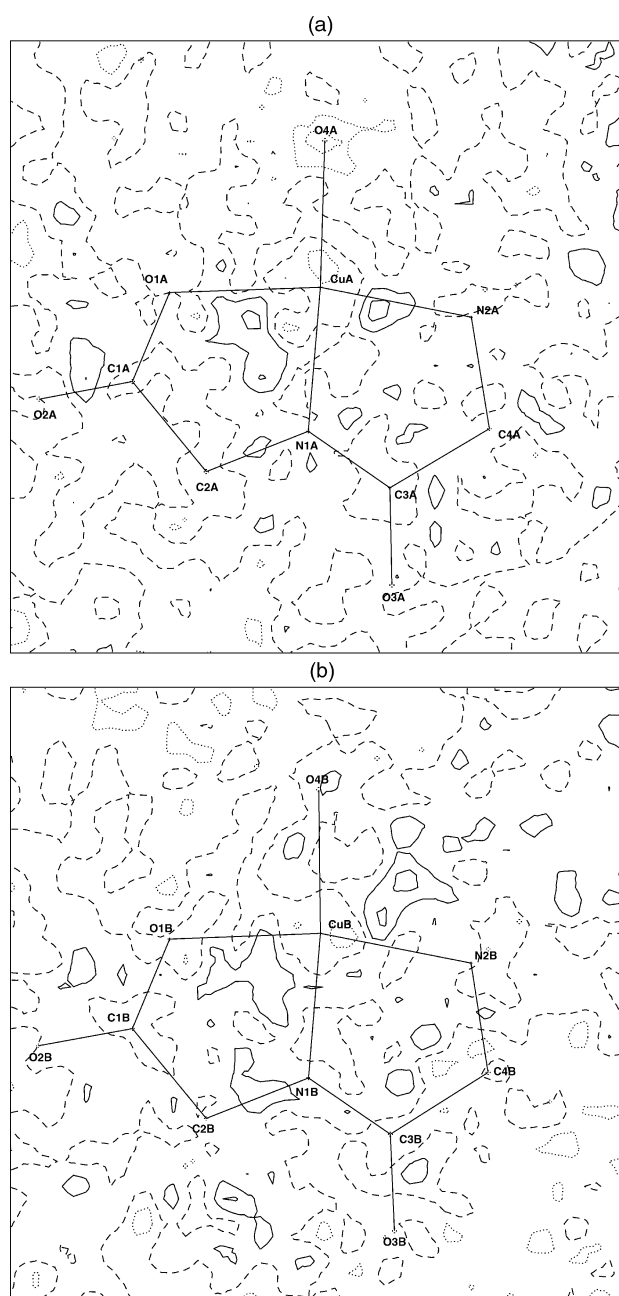


Fig. 3 XD residual density maps for Cu(glygly)(OH)₂·H₂O in the Cu-glygly-O4 best-fit plane. The contours are at 0.2 e Å⁻³, solid lines positive, dashed lines negative. (a) Molecule A. (b) Molecule B.

atomic orbitals adapted for the chemical environment of an atom form the basis. The program ASRED,¹² as recently updated,¹³ was employed. Hydrogen atom positions were refined. The copper atoms were allowed 3d valence orbital functions, with a “mixing” coefficient between the approximate *t*_{2g} and *e*_g orbital sets and a diffuse 4s-like function. The oxygen,

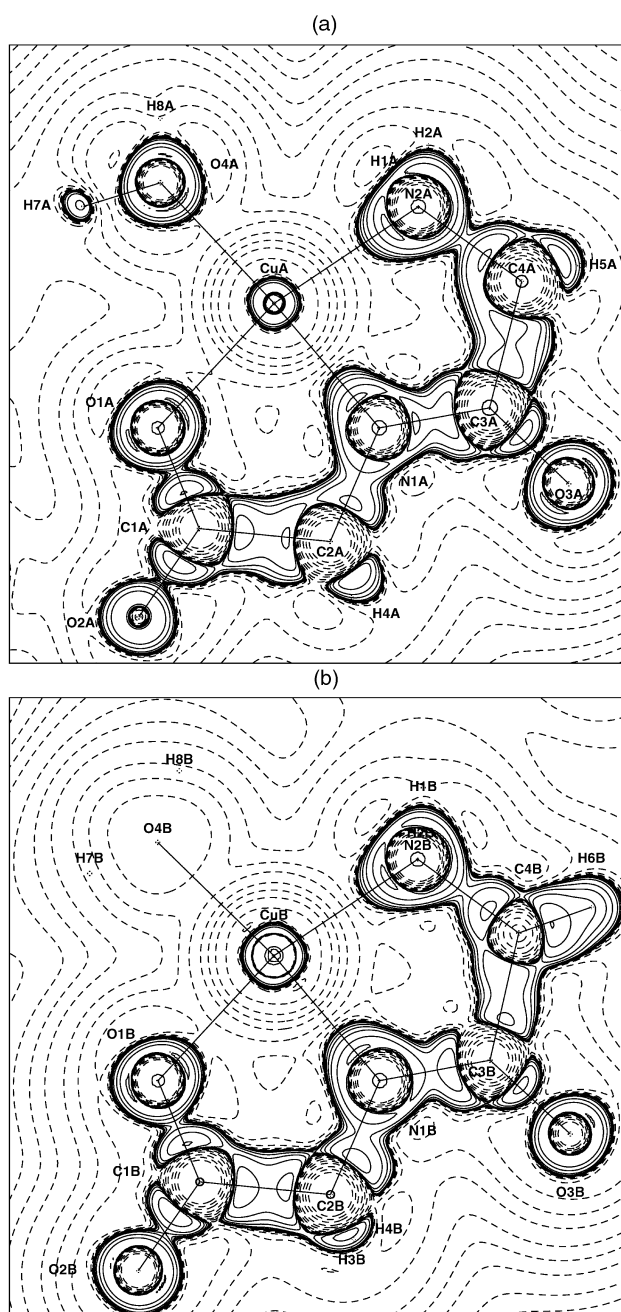


Fig. 4 XD *L*(ρ) maps for Cu(glygly)(OH)₂·H₂O in the Cu-glygly-O4 best-fit plane. Contours are at zero and ±(0.002, 0.004, 0.008) × 10⁻², *n* = 0 to 5, e Å⁻⁵; solid lines positive (charge locally concentrated), dashed negative (charge locally depleted). (a) Molecule A. (b) Molecule B.

nitrogen and carbon atoms had (sp³), (sp²) + *p*_π, or (sp) + 2*p*_π functions as appropriate to their chemical binding. For each such atom a single *κ* variable modified the valence form factor. The hydrogen atoms were allowed the single 1s function¹¹ whose form factor was not refined. Again, the form factors were

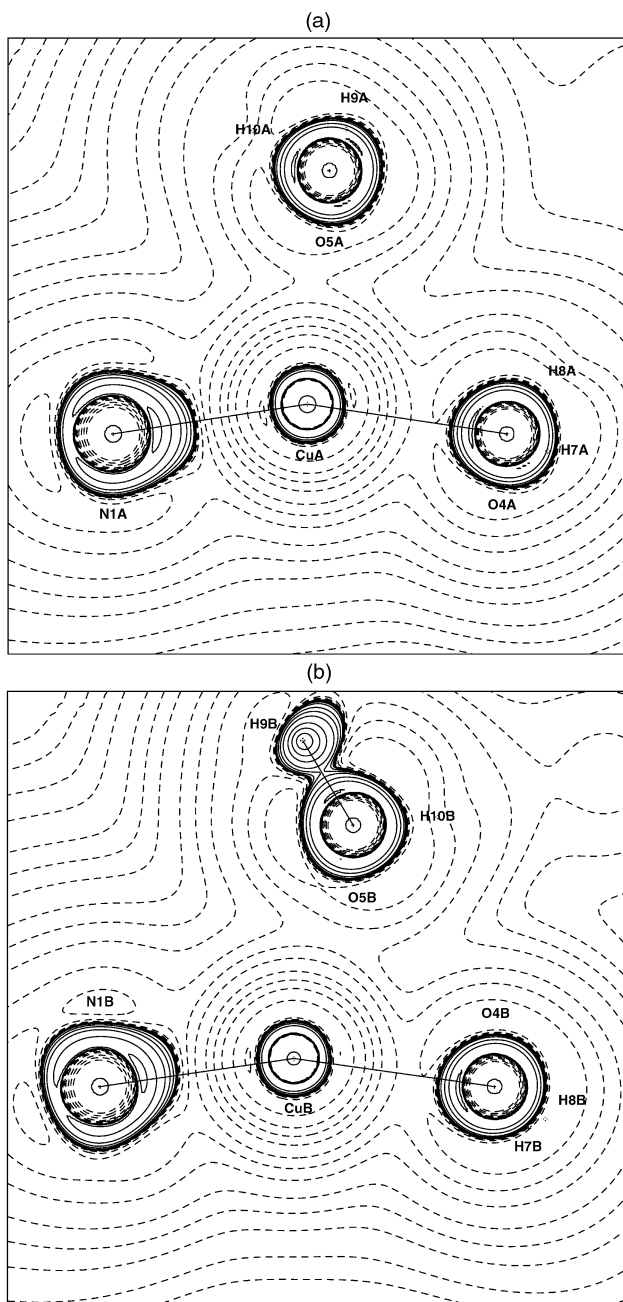


Fig. 5 XD Laplacian of the density maps for $\text{Cu}(\text{glygly})(\text{OH}_2)_2 \cdot \text{H}_2\text{O}$ in the O4–Cu–O5 plane. Contours are as for Fig. 4. (a) Molecule A. (b) Molecule B.

derived from appropriate sets of Clementi and Roetti constants.¹⁰ A parameter to model multiple scattering as an additional constant term in the intensity was included.¹⁴ Details of the refinement are given in Table 2. The positional and the equivalent ADP are presented in Table S1 (ESI). The anisotropic ADP and the $F_{\text{obs}}/F_{\text{calc}}$ are deposited in Tables S3h,i. The hybrid orbital populations are presented in Table 3.

Topological analysis

Examination of the topological properties of the experimental electron density was undertaken using the atoms-in-molecules (AIM) approach of Bader.¹⁵ The PROPERTIES package of the XD program was used to find bond critical points (bcp) and the values of charge density (ρ) and the Laplacian ($-\nabla^2\rho$) at those entities. The program TOPXD¹⁶ was employed to integrate over the atomic volumes defined by the zero-flux-density surfaces.¹⁵ The integrations were performed using a radial grid that

was as fine as we could afford in view of the size and complexity of the molecule. Reasonable precision of all the integrations was obtained, as measured by the atomic Lagrangian,¹⁶ which ideally should be zero. Values of the Lagrangian were mostly about 10^{-3} a. u., but were as low as 10^{-5} a. u. in some cases.

For reference, a theoretical calculation at the MP2/6-31G* level was performed on an isolated $\text{Cu}(\text{glygly})(\text{OH}_2)_2$ molecule with the relative atomic positions of Molecule A with the Gaussian98 software.¹⁷ Topological analysis of the electron density produced by this calculation was carried out with the MORPHY98¹⁸ software.

Results

Details of the ambient temperature and 10 K spherical atom, the multipole and the valence orbital refinements are given in Table 2. Fig. 1 illustrates the two independent $\text{Cu}(\text{glygly})(\text{OH}_2)_2$ molecules with the numbering scheme employed and Fig. 2 the unit cell contents. The fractional atomic positions, bond lengths and angles, anisotropic ADP and the XD multipole coefficients and their reference axes are set out in the ESI. The valence orbital population parameters and associated information are presented in Table 3. Atomic charges deduced by various procedures are listed in Table 4. Topological information at bond critical points is presented in Table 5.

Discussion

Geometry of $\text{Cu}(\text{glygly})(\text{OH}_2)_2$

The unit cell contains $\text{Cu}(\text{glygly})(\text{OH}_2)_2$ molecules and uncoordinated water molecules. These latter water molecules have an important role in the extensive hydrogen bonding which stabilises the crystal structure, but we do not follow that further here. The copper atoms are 5-coordinate, but one of the two water molecules involved has a much larger Cu–O distance than has the other; Cu–O5 2.3 Å *versus* Cu–O4 1.96 Å. The Cu–O5 bond lengths also differ between the molecules of types A and B (0.06 Å) whereas Cu–O4 is much more consistent (0.01 Å) and much closer to the glygly ligand donor oxygen value (Cu–O1, 1.98 Å). It appears that the O5 water molecule is more loosely held by its associated copper atom than is that of O4.

Roughly, O4 and the donor atoms of the ligand form a square plane, the Cu atom lies about 0.2 Å above this, with the O5 water molecule only approximately in the apical position of a square pyramid, and varying between the two types of molecule. The arrangement is shown in Fig. 1. The molecular geometry is close to that predicted for $\text{M}(\text{tridentate})(\text{unidentate})_2$ systems by simple donor atom repulsion theory.¹⁹ In the nomenclature used there, the experimental N2–N1–O1 angle is 100.2° (100°) and the normalised bite 1.32 (1.2), where the values in parentheses are those predicted.

Apart from the distance and position of the O5 water molecule, the two types of complex ion in the crystal have very similar geometrical features. At 10 K the Cu–X bonds, X = O4, O1, N1, N2 differ by more than 0.01 Å only for the N2 case, where the difference is 0.02 Å. The X–Cu–X' angles differ by less than 1° except for one of those involving the rather more loosely held N2 atom where a 3.5° difference (O4) is observed. Within the glygly ligand itself the bond lengths are the same within 0.01 Å and the angles within 1.0°.

At O1 the Cu–O1–C1 angle is 115°, which is midway between the 109.5° of tetrahedral geometry and the 120° of trigonal stereochemistry. At N1 the Cu–N1–C2 and Cu–N1–C3 angles are 116.5 and 119.7° respectively, fairly close to trigonal symmetry. At N2 the Cu–N2–C4 angle is 109.7°, close to the tetrahedral value. At C1 the O2–C1–O1 and O2–C1–C2 angles are 123.4 and 117.8° respectively, indicating trigonal geometry. The same applies for C3 where the angles are O3–C3–N1, 126.4° and O3–C3–C4, 119.6°.

Table 3 Valence orbital population parameters (e) and related information for non-hydrogen atoms in Cu(glygly)(OH)₂·H₂O at 10 K

										k^a	x^b	z^b
Cu(A)	d_{xy}		1.58(3);	d_{xz}	1.61(3);	d_{yz}	1.68(3);	$d_{x^2-y^2}$	1.78(3)			
(B)	d_{z^2}		1.17(3);	'4s'	2.2(3);					0.84(1)	N2	N1
			1.74(3);		1.59(3);		1.57(3);		1.65(3)			
			1.16(3);		1.1(3)					0.83(1)		
O4(A)	(sp ³)	1	1.67(3);	2	1.45(4);	3	1.67(3);	4	1.48(4)	1.00(1)	O5	Cu
(B)			1.69(3);		1.46(4);		1.65(3);		1.64(4)	1.01(1)		
O5(A)	(sp ³)	1	1.64(3);	2	1.58(4);	3	1.64(3);	4	1.61(4)	1.01(1)	O4	Cu
(B)			1.70(3);		1.55(4);		1.48(3);		1.66(4)	1.01(1)		
O1(A)	(sp ³)	1	1.71(3);	2	1.75(4);	3	1.74(3);	4	1.50(3)	1.02(1)	C1	Cu
(B)			1.77(3);		1.71(4);		1.62(3);		1.58(3)	1.02(1)		
N1(A)	(sp ²)	1	1.53(4);	2	1.41(4);	3	1.50(4);	p_π	1.25(4)	1.04(1)	C2	Cu
(B)			1.57(4);		1.51(4);		1.52(4);		1.25(4)	1.05(1)		
N2(A)	(sp ³)	1	1.55(4);	2	1.36(4);	3	1.27(4);	4	1.39(5)	1.02(1)	C4	Cu
(B)			1.57(4);		1.41(4);		1.29(4);		1.24(5)	1.01(1)		
O2(A)	(sp)	1	1.82(4);	2	1.75(4);	$2p_\pi$	2.97(8);			1.04(1)	C1	O1
(B)			1.78(4);		1.82(4);		2.99(8);			1.04(1)		
O3(A)	(sp)	1	1.63(4)	2	1.59(3);	$2p_\pi$	3.27(8);			1.04(1)	C3	N1
(B)			1.71(4)		1.69(3);		3.24(8);			1.06(1)		
C1(A)	(sp ²)	1	1.02(5)	2	1.07(5);	3	1.10(5);	p_π	0.39(5)	0.94(1)	O2	O1
(B)			0.91(5);		0.91(5);		0.99(5);		0.51(5)	0.95(1)		
C2(A)	(sp ³)	1	1.24(5);	2	0.99(5);	3	1.06(6);	4	1.03(6)	1.03(1)	C1	N1
(B)			1.18(5);		0.88(5);		0.92(6);		0.95(6)	0.97(1)		
C3(A)	(sp ²)	1	1.07(5);	2	1.16(5);	3	1.07(6);	p_π	0.39(5)	0.96(1)	O3	N1
(B)			0.95(5);		1.05(5);		0.90(6);		0.46(5)	0.93(1)		
C4(A)	(sp ³)	1	1.38(5);	2	0.93(5);	3	1.00(6);	4	1.05(6)	1.02(1)	C3	N2
(B)			1.32(5);		0.87(5);		0.93(6);		0.71(6)	0.93(1)		
O6(A)	(sp ³)	1	1.40(5);	2	1.25(6);	3	1.56(3);	4	1.57(3)	0.98(1)	H2	H1
(B)			1.48(5);		1.29(6);		1.64(3);		1.61(3)	0.99(1)		

^a The form factor is calculated at κr rather than at r ; $\kappa > 1$ corresponds to a contraction of the electron density in real space. ^b z is defined along the vector along the line from the row-atom to the z -atom; x lies in the plane defined by z and vector from the row-atom to the x -atom, perpendicular to z , and near that vector.

Multipole refinement

As measured by the reliability indices listed in Table 2, the XD multipole treatment of the 10 K data produced a better refinement than the spherical atom model, as expected. Owing to the different weighting schemes of the spherical atom on the one hand and the multipole and valence-orbital (identical) refinements on the other, the goodness-of-fit cannot be used for the comparison of the two types of refinement, as would be desirable. There are, of course, many more parameters varied in the multipole approach, and not all are significant relative to their least-squares uncertainties. The parameters show quite good agreement between the two types of Cu(glygly)(OH)₂ complexes, but they are not chemically transparent, and are not discussed further here. For our purposes the main value of the XD refinement is that it provides a basis for a topological analysis of the experimental charge density within the AIM approach.¹⁵

Valence orbital refinement

The application of the ASRED refinement procedure makes assumptions about atom site symmetry in order to obtain chemical transparency. In that way it is possible to reduce the number of variable parameters relative to a multipole model and to couch these parameters in chemically relevant terms. The assumptions involved, of course, bring a reduction in rigor. However, it is usually possible to obtain almost as good a fit to the data as from the multipole treatment, as can be seen here in Table 2.

In the present case, the ASRED procedure reduces the number of valence parameters (populations and κ -values) of the multipole model, from 562 to 160. Apart from the conditions set out in the Refinements section above, the following assumptions were made about the valence hybridisations of the non-copper and non-hydrogen atoms, based upon the bond angles discussed in the Geometry section above:

non-carbonyl O; O1, O(4–6)	tetrahedral (sp ³)
carbonyl O; O2, O3	linear (sp) + $2p_\pi$
secondary amine; N1	trigonal (sp ²) + p_π
primary amine; N2	tetrahedral (sp ³)
methylene C; C2, C4	tetrahedral (sp ³)
carbonyl C; C1, C3	trigonal (sp ²) + p_π

From the Geometry section the argument that O1 should be treated as tetrahedral rather than trigonal is not clear since the Cu–O1–C1 angle is 115°, but as little Cu–O π -bonding seems likely, that choice was made.

Agreement between valence orbital parameters

The valence orbital population parameters on the atoms of the molecules labelled A and B in Table 3 show encouraging agreement, except, as is usual, for the diffuse '4s' component on copper. The average Cu d-orbital disagreement is 0.08 (max 0.16) e and the average oxygen and nitrogen atom s,p disagreement is 0.06 (max 0.16) e. On the carbon atoms the result is poorer, with an average disagreement of 0.09 e dominated by a single difference of 0.34 e located on C4. These disagreements are about twice as large as the least-squares errors attached to the parameters.

These results provide a direct guide to the reliability of the determination of valence features by X-ray diffraction techniques, and confirm the impression gained from previous studies that the populations are consistent to 0.1 e or better and that the least-squares errors involve serious underestimates.

The κ -values associated with the populations also show encouraging agreement; for Cu κ_{3d} differs by only 0.01 between the A and B molecules, for the oxygen and nitrogen atoms the average s,p disagreement is less than 0.01 (max 0.02), but for the carbon atoms it is 0.05. Again, the account for the carbon atoms is much less consistent.

Table 4 Formal charges on atoms and on water molecules in Cu(glygly)(OH)₂·H₂O deduced by different procedures. For the hydrogen atoms the label in parentheses refers to the attached atom to improve clarity

	CuA	CuB	O4A	O4B	O5A	O5B	O1A	O1B	N1A	N1B	N2A	N2B	O2A	O2B	O3A	O3B
Stockholder	−0.39	−0.35	0.19	0.25	0.08	0.00	−0.08	−0.94	−0.47	−0.46	−0.35	−0.44	0.13	−0.10	−0.40	0.03
Monopole	2.8	2.8	0.18	0.21	0.14	0.18	0.37	0.32	0.11	0.13	0.02	−0.10	0.36	0.30	0.33	0.34
Valence Orb.	1.0	2.1	−0.28	−0.59	−0.49	−0.40	−0.71	−0.69	−0.70	−0.89	−0.57	−0.51	−0.55	−0.59	−0.49	−0.64
AIM	0.23	0.22	−0.87	−0.91	−0.91	−0.83	−1.10	−1.19	−1.62	−1.32	−1.03	−1.03	−1.13	−1.28	−0.84	−0.92

	C1A	C1B	C2A	C2B	C3A	C3B	C4A	C4B	O6A	O6B	H1(N2)A	H1(N2)B	H2(N2)A	H2(N2)B	H3(C2)A	H3(C2)B
Stockholder	−0.15	−0.36	−0.27	−0.37	0.00	0.15	0.18	0.31	0.31	0.40	—	—	—	—	—	—
Monopole	−1.30	1.50	−0.60	−0.80	−0.80	−0.60	−0.70	−1.10	0.29	0.27	0.08	0.11	0.20	0.18	−0.08	0.11
Valence Orb.	0.43	0.72	−0.31	0.07	0.31	0.60	−0.37	0.17	0.22	0.03	0.12	0.16	0.18	0.01	−0.08	−0.06
AIM	0.97	0.82	−0.02	−0.02	0.90	1.43	−0.18	−0.87	−0.74	−0.70	0.40	0.31	0.55	0.49	−0.14	0.09

	H4(C2)A	H4(C2)B	H5(C4)A	H5(C4)B	H6(C4)A	H6(C4)B	H7(O4)A	H7(O4)B	H8(O4)A	H8(O4)B	H9(O5)A	H9(O5)B	H10(O5)A	H10(O5)B	H11(O6)A	H11(O6)B
Stockholder	—	—	—	—	—	—	—	—	—	—	—	—	—	—	—	—
Monopole	0.06	0.15	0.13	0.13	0.09	0.19	0.12	0.15	0.13	0.13	0.11	0.17	0.19	0.12	0.16	0.23
Valence Orb.	−0.03	−0.07	0.02	−0.11	−0.09	−0.02	0.27	0.29	0.33	0.26	0.25	0.27	0.24	0.19	0.23	0.16
AIM	0.03	0.12	0.18	0.12	0.07	0.24	0.60	0.62	0.61	0.69	0.63	0.64	0.64	0.68	0.68	0.71

	H12(O6)A	H12(O6)B	H ₂ O4A	H ₂ O4B	H ₂ O5A	H ₂ O5B	H ₂ O6A	H ₂ O6B
Stockholder	—	—	—	—	—	—	—	—
Monopole	0.22	0.13	0.43	0.49	0.44	0.47	0.67	0.63
Valence Orb.	0.24	0.14	0.32	−0.04	0.00	0.06	0.69	0.33
AIM	0.66	0.57	0.34	0.40	0.36	0.49	0.60	0.58

Table 5 Electron densities (ρ) ($\text{e } \text{\AA}^{-3}$) and the Laplacian ($L_c(\rho) = -\nabla^2(\rho)$) ($\text{e } \text{\AA}^{-5}$) at the bond critical points in $\text{Cu}(\text{glygly})(\text{OH}_2)_2 \cdot \text{H}_2\text{O}$. ρ_A^{th} and $L_c(\rho)_A^{\text{th}}$ refer to the theoretical calculation with the relative atom positions of molecule A

Bond	ρ_A	ρ_B	ρ_A^{th}	$L_c(\rho)_A$	$L_c(\rho)_B$	$L_c(\rho)_A^{\text{th}}$
Cu–O4	0.60	0.60	0.55	−10.4	−9.8	−9.7
Cu–O5	0.29	0.28	0.29	−4.1	−3.2	−4.5
Cu–O1	0.66	0.68	0.57	−9.8	−9.6	−7.5
Cu–N1	0.81	0.80	0.79	−11.6	−12.8	−8.8
Cu–N2	0.74	0.74	0.58	−6.9	−7.1	−6.6
O1–C1	2.51	2.61	2.36	33.7	32.6	−0.4
O2–C1	2.52	2.62	2.55	15.2	30.4	4.1
O3–C3	2.33	2.19	2.43	30.3	18.5	8.6
N1–C2	1.90	1.89	1.82	21.4	17.7	19.3
N1–C3	2.42	2.37	2.45	11.4	33.0	20.5
N2–C4	1.56	1.78	1.66	8.7	13.8	16.0
C1–C2	1.79	1.86	1.74	15.9	18.2	15.5
C3–C4	1.77	1.80	1.75	21.2	12.6	15.8

Atomic charges

The concept of the charge on an atom bound to other atoms does not have a sound physical base, but nevertheless continues to attract chemical interest. Atomic charges from X-ray data have been obtained mainly by the Stockholder method²⁰ and by the monopole populations of a multipole refinement. The sums of valence orbital populations have also been used.^{21–23} Although these methods have recognised limitations which mean the absolute values they produce are not reliable, they have often been used to examine trends amongst atoms of a given type in different chemical environments, and we do that here. In view of the crudeness of the results, it was not considered meaningful to use the Stockholder method to assess the charges of the hydrogen atoms.

The Bader AIM approach¹⁵ offers a more respectable possibility, at least from the point of view of quantum mechanics. It has been employed to analyse electron densities corresponding to the wave functions of theoretical calculations, but unfortunately there are considerable technical difficulties in applying it to densities derived from the structure factors of an X-ray experiment,²⁴ and the calculations required are lengthy. Recent publications^{16,25,26} describe work in this area. The program TOPXD¹⁶ has been made available to us and we have extended its application to the present $\text{Cu}(\text{glygly})(\text{OH}_2)_2 \cdot \text{H}_2\text{O}$ data.

It is often found in studies such as the present that the charges on appropriate groups of atoms are conserved more consistently than are those of the individual atoms. In that vein, the charges on the water molecules associated with O4, O5 and O6 also are listed in Table 4.

Stockholder charges. For $\text{Cu}(\text{glygly})(\text{H}_2\text{O})_2 \cdot \text{H}_2\text{O}$ the Stockholder partitioning yields formal charges that have modest consistency between molecules A and B (Table 4), but no chemical relevance. The charges deduced are all relatively small, less than unity. The copper atoms come out negatively charged, the oxygen and carbon atoms both show both positive and negative values, while the nitrogen atoms are the most negative. They are not discussed further.

Multipole monopole charges and dipole moments. The monopole charges of 2.8 e for the copper atoms, given in Table 4, although consistent between molecules A and B, are chemically unacceptable. The monopole charges on the oxygen atoms agree fairly well between molecules A and B, and are all small and positive (0.14 to 0.37 e) and so do not conform with chemical expectations. The expected shift of electrons onto these electronegative atoms is not seen. The nitrogen atom charges also do not conform with expectations for an electronegative atom, with both N1 and N2 little different from zero (−0.10 to 0.13 e). The carbon atoms agree less well between the two mole-

cules and they deviate from chemical sense in that they are mostly negative (−1.3 to 1.5 e) although attached to more electronegative oxygen and nitrogen atoms. The hydrogen atom charges are mostly quite small and positive (−0.02 to 0.65 e), and there is no obvious correlation with the electronegativity of the attached atom. Altogether, it seems that the monopole populations are not valuable in even tracing trends in this study.

The charges of the water molecule show good consistency between atom sets A and B, with an average difference 0.04 e. The molecules based on O4 and O5, bound to the copper ion, have essentially the same charge, 0.46(1) e, and this is distinctly lower than that of 0.65 e on the “free” O6 based molecule. It seems that indeed, at least for these water molecules, group monopole charges are more reliable than those of individual atoms.

The multipole refinement results also allow the possibility of calculating effective dipole moments for groups of atoms, although charged, by using an established charge scaling procedure.²⁷ The method was applied here to the three water molecules in the structure, $\text{H}_2\text{O4}$ and $\text{H}_2\text{O5}$ bonded to Cu and “free” $\text{H}_2\text{O6}$, to examine whether the dipole moment might reflect their bonding situation. The dipole moment of the gaseous H_2O molecule is 6.16×10^{-30} C m. The values obtained were: $\text{H}_2\text{O4}$ (7.5, 6.2), $\text{H}_2\text{O5}$ (2.8, 5.5) and $\text{H}_2\text{O6}$ (5.4, 5.1) C m $\times 10^{-30}$. The pairs of numbers within parentheses are respectively for atom sets A and B. Since the dipole moment of the “free” water molecule, close to that of the gaseous molecule, lies between those for the two bonded molecules, no correlation between that property and the amount of interaction with the copper ion is apparent. Perhaps the much larger disagreement between the A and B atom sets for the $\text{H}_2\text{O5}$ case arises because of the relatively large difference (0.06 Å) in Cu–O5 bond lengths.

Valence orbital charges. The valence orbital based charges of Table 4 make somewhat more sense than those of the Stockholder and monopole analyses, but are still scarcely sufficient to be of chemical value. Although the agreement between molecules A and B for the copper atom is poor because the ‘4s’ component is not well defined, the average result of +1.5 e is reasonable. The poor accuracy of the ‘4s’ population arises because its diffuse nature means that it is defined by only a relatively few reflections at low values of 2θ , and these, although possibly quite intense, then tend to be affected by extinction.

The oxygen atoms are negatively charged, except for O6 of the ‘free’ water molecule, with fair agreement between values for the two molecules (average disagreement 0.15 e). No difference between types of oxygen atom, *viz.* the water molecules, the glygly-O1 and the carbonyl-O atoms, can be distinguished. The average charge is −0.43 e. The nitrogen atoms are, on average, more negative than the oxygen atoms, −0.67 e, with somewhat better consistency. The carbon atoms are less consistent than the oxygen atoms between A and B molecules, but range from negative to positive, with an average charge of +0.20 e.

The hydrogen atoms show good consistency between the two molecules, with an average disagreement of 0.07 e. The charges are mostly small (−0.07 to 0.52 e) but there is some correlation with the electronegativity of the attached atom: average charge for H(O) = 0.24, for H(N) = 0.12, for H(C) = −0.04 e.

Thus, overall, the copper atom has, as expected, somewhat less than the formal +2 charge, the electronegative oxygen and nitrogen atoms are indeed negatively charged, but O less than N, and the carbon atoms are near neutral, as expected. The hydrogen charges are small, as is reasonable, and vary sensibly with the electronegativity of the attached atom.

In contrast to the monopole results, the water molecule charges show rather poor consistency between atom sets A and B, with an average difference of 0.26 e. The molecules based

on O4 and O5, bound to the copper ion, have an average charge 0.09(5) e, and this, in spite of the poorer overall agreements, is significantly lower than that of 0.51 e on the “free” O6 based molecule. This was seen also for the monopole based charges.

Atoms-in-molecules charges. The AIM charges generally agree better between the two molecules A and B than for the other methods of charge assessment. For example, the average disagreement of the oxygen atoms is 0.08 e and for the copper atoms it is only 0.003. For the trigonal nitrogen atoms and the carbon atoms of the ligand the difference is larger, as much as 0.4 e. Of course, some inequalities must be expected on account of the non-vanishing differences in bond lengths and angles of the two molecules. However, although there are some interesting agreements, overall the charges do not conform to chemical expectations any better than do those from the valence orbital populations.

The copper atoms have the small positive charge of about 0.2 e, which might be thought to be rather low as, for example, topological analysis of the theoretical calculation results for an isolated molecule leads to a copper atom charge of +1.21 e.

The average oxygen atom charge is -0.95 e, which is very sensible but is not as negative as that of the less electronegative nitrogen atoms, average -1.25 e. There is some consistency with chemical environment in that O1 and O2 of the carboxyl group are the most negative (≈ -1.2 e) and O6 of the isolated water molecule is the least negative (-0.7 e). The O4 and O5 of the two coordinated water molecules together with the carbonyl O3 all have a charge of about -0.9 e, with the longer Cu–O bond length for O5 relative to O4 apparently having no effect.

The nitrogen atoms are the most negative and show marked differences between members, with the trigonal amido N1 -1.5 and the amino N2 -1.0 e. For reference, topological analysis of the experimental X-ray data for NH_3 using TOPXD yielded an AIM integrated charge²⁸ of -1.5 e for the nitrogen atom.

Although there is a relationship with chemical environment, the carbon atom charges are very varied, -0.87 to 1.43 e, and some are chemically unacceptable. C1 and C3 of the C=O groups have the positive charge expected for binding to the electronegative oxygen atoms, but it seems unreasonably large at ≈ 1.0 e. The charges of the methylene carbon atoms C2 and C4, bound to a nitrogen and another carbon atom, are slightly negative, average ≈ -0.3 e, whereas a similar positive result might have been expected.

The hydrogen atom charges larger than the multipole and V. O. results show an interesting correlation with the electronegativity of their attached atom with, as averages: $\text{H}(\text{O}) = 0.64$, $\text{H}(\text{N}) = 0.44$ and $\text{H}(\text{C}) = 0.09$ e. For reference, from experiment the integrated AIM charges for hydrogen in oxalic acid hydrate²⁹ were 0.3 (OH) and 0.4 (OH_2) e and for NH_3 0.5 e.²⁸ For the amino H atoms of *p*-nitroaniline 0.47 e was deduced.¹⁶ From a series of *ab-initio* calculations in a variety of $\text{A}(\text{OH})_n$ molecules³⁰ ($\text{A} = \text{Be}, \text{B}, \text{C}$) the hydrogen atom charges ranged from 0.42 to 0.69 e. Thus the results of Table 4 for hydrogen atoms are not unusual.

As for the monopole results, although not to the same extent, the water molecule charges show good consistency between atom sets A and B, with an average difference 0.04 e. The molecules based on O4 and O5, bound to the copper ion, have an average charge 0.40(3) e, and this again is significantly lower than that of 0.59 e on the “free” O6 based molecule, as for the monopole and valence orbital cases.

Valence orbital populations

Although, as seen in the preceding section, the total valence orbital populations on various atoms do not define atomic charges well, their relative values are quite informative.

On copper, the ‘4s’ populations do not merit discussion, but the 3d values of Table 3 are useful. When the $\text{Cu}(\text{glygly})(\text{OH})_2$

molecule is approached from the point of view of ligand field theory the obvious description is as an ‘octahedral’ complex in which one ligand, that opposite to the O5 water molecule, has been ‘lost’. Since the coordinate axis system on copper was chosen with z along the Cu–N1 direction (approximately O4–Cu–N1) a simple ligand field theory treatment predicts that, for the relevant d^9 configuration, the ‘hole’ in the d^{10} shell should be in the d_{z^2} orbital, with the other four 3d orbitals filled. This is indeed seen in broad terms; the d_{xy} , d_{xz} , d_{yz} and $d_{x^2-y^2}$ orbital populations average 1.65 e (mean deviation 0.06 e), while for d_{z^2} the average is 1.16 e.

For the oxygen atoms there is good agreement between individual orbital populations for molecules A and B, with a mean difference of 0.06 e. However, within a given oxygen atom no particular pattern is apparent between the populations of different sp hybrid orbitals, or for that matter the p_π orbitals of the carbonyl oxygens O2 and O3. The average deviation from the mean of 1.60 e is 0.10 e, so that they are equally populated. However, since the orbitals are all nearly fully occupied (1.5 to 1.8 e) any differences could not be expected to be large. As shown by the charges discussed above, there is a distinctly lower overall population on O6 of the ‘free’ water molecule and a slightly higher one on the glygly oxygen O1, but no large difference amongst the values within each. The longer Cu–O5 bond relative to Cu–O4 presumably reflects a looser attachment of the O5 water molecules, but this is not reflected in the respective hybrid orbital populations. Within the carbonyl oxygens, O2 and O3, the two p_π orbitals are populated equally with the two (sp) hybrids.

The position for the nitrogen atoms N1 and N2 is similar to that for the oxygens. The mean difference between molecules A and B is 0.05 e and the average deviation of the sp^n and p_π populations from the mean of 1.41 e is 0.11 e. The p_π orbital on N1 may be less populated than the sp^2 hybrids but the effect is scarcely at a level of significance. The populations of the four orbitals add up to about 0.8 e less than is the case for the oxygen atoms and that, of course, reflects the fact that nitrogen has one fewer valence electrons than has oxygen, and a relatively similar electronegativity.

Although the definition of the carbon atoms is poorer, the mean population difference between molecules A and B being 0.12 e, on the C1 and C3 carbonyl-C atoms there is a feature of interest. Over all the sp^n hybrids of C1–C4 the average population is 1.02 e, with a mean deviation of 0.11 e, as for the oxygen and nitrogen atoms. However, the p_π populations of C1 and C3 are much lower, 0.44 e with a mean deviation of 0.05 e. It seems that here we are able to see clearly the concentration of electrons into the σ -bonding system on the carbonyl carbon atoms at the expense of a weaker π -bonding system. The four valence orbital populations sum to about 2.3 e less than for the oxygen atoms, consistent with the two fewer valence electrons and the lower electronegativity of carbon.

Topological analysis

Electron densities at bond critical points. The PROPERTIES facility of the XD program was able to locate bond critical points (bcp) in the electron density of the $\text{Cu}(\text{glygly})(\text{OH})_2$ molecules for all the relevant non-hydrogen atom interactions, as shown in Table 5. It also located the topologically necessary ring critical points. The agreement of the values for the densities at these points for the bonds in molecules A and B is quite good, with an average difference of 3%. There is also modest agreement with the theoretical values calculated for molecule A for nearly all the bonds. The experimental bcp densities in the Cu–O and Cu–N bonds are in the range 0.3 to $0.8 \text{ e } \text{\AA}^{-3}$. Experimental values have been reported for few other metal–donor atom systems. The most relevant seem to be 0.65 and $0.76 \text{ e } \text{\AA}^{-3}$ for Ni–N bonds,³¹ 0.46 [0.52] $\text{e } \text{\AA}^{-3}$ for Co–As bonds,³² 0.93 [0.91] $\text{e } \text{\AA}^{-3}$ for Co–C bonds and 0.55 for

Ni–C bonds³³ (figures in square brackets are from theoretical calculations). These values are all consistent with bonding which is of mixed ionic/covalent character.³² The experimental values we obtained seem reasonable in this light. The bcp density for Cu–O5 (average $0.29 \text{ e } \text{\AA}^{-3}$) is distinctly lower than that for the Cu–O4 and Cu–O1 bonds (average $0.64 \text{ e } \text{\AA}^{-3}$) and this is significant and presumably reflects the weakness of the longer Cu–O5 bond.

The O–C, O=C, N–C and C–C bcp densities are larger than those involving Cu, ranging from 1.6 to $2.6 \text{ e } \text{\AA}^{-3}$. The higher values are consistent with the largely covalent nature of the bonding here. Some relevant experimental results for transition metal complexes for comparison are: $3.6 \text{ e } \text{\AA}^{-3}$ for N=O bonds,³¹ $3.4 \text{ e } \text{\AA}^{-3}$ for C=O bonds³³ and 1.7 to $2.6 \text{ e } \text{\AA}^{-3}$ for C–C bonds.³² Results from several charge density studies of metal-free small peptide compounds have been presented and reviewed along with others from the literature.^{34,35} There is seen to be rather good consistency in ρ_c for all these bonds. The bonds lay in the ranges now given; the figures in parentheses are from our present study and those in square brackets from a theoretical calculation.^{34,35} O–C bonds 2.38 to 3.02 (2.65) [$—$] $\text{e } \text{\AA}^{-3}$, O=C bonds 2.59 to 2.96 (2.53) [2.75] $\text{e } \text{\AA}^{-3}$, N–C(H₂) bonds 1.70 to 1.90 (1.80) [1.88] $\text{e } \text{\AA}^{-3}$, N–C(O) bonds 2.25 to 2.46 (2.34) [2.26] $\text{e } \text{\AA}^{-3}$, and C–C bonds 1.65 to 1.80 (1.80) [1.88] $\text{e } \text{\AA}^{-3}$.

Laplacian at the bond critical point. The Laplacian, $L(\rho) = -\nabla^2\rho$, provides a sensitive and informative probe of chemical bonding features, particularly at a bcp¹⁵ ($L_c(\rho)$). Analysis of theoretically generated densities shows that covalent bonding leads to large positive values of $L_c(\rho)$ and ionic bonding to negative values. Experimental results reflect this, although quantitative agreement with theoretical values is not obtained.

For the Cu(glygly)(OH)₂ molecules the agreement in the Laplacian between molecules of A and B types at the Cu–O and Cu–N bcp's is reasonably good, and the values, $L_c(\rho) = -3$ to $-13 \text{ e } \text{\AA}^{-5}$, fall in the range found by experiment for other M–L systems, and reflect a mixed ionic/covalent situation. For example, $L_c(\rho)$ has been reported as $-5 \text{ e } \text{\AA}^{-5}$ for Ni–C bonds,³³ $\approx -8 \text{ e } \text{\AA}^{-5}$ for Ni–N bonds,³¹ $-4 \text{ e } \text{\AA}^{-5}$ for Co–As bonds,³² and $-12 \text{ e } \text{\AA}^{-5}$ for Co–C bonds.³² We find $L_c(\rho)$ for the Cu–O5 bonds ($-3.6 \text{ e } \text{\AA}^{-5}$) is much smaller in magnitude than for the other Cu–O and Cu–N bonds (average $-9.8 \text{ e } \text{\AA}^{-5}$, mean deviation $1.9 \text{ e } \text{\AA}^{-5}$) and this, as for the density discussed in the previous section, presumably reflects the weakness of the longer Cu–O5 bond. The agreement with the theoretical values for molecule A is little better than qualitative.

The C–C bonds, of course, are the most covalent and they indeed have large positive values of $L_c(\rho)$, 13 to $21 \text{ e } \text{\AA}^{-5}$. The large scatter amongst their values has also been noted in other studies involving C–C bonds in transition metal complexes; for example, 11 to $22 \text{ e } \text{\AA}^{-5}$ has been found.³³ The Laplacian is obviously very sensitive to the detail of the electron distribution in highly covalent systems.

The more polar, but still largely covalent O–C and N–C bonds mostly show values of $L_c(\rho)$ larger than those for the Cu–L bonds and even larger than for the C–C bonds. They range from 9 to 34 , average 22 , $\text{e } \text{\AA}^{-5}$. The values agree modestly between molecules A and B but there is large scatter and one cannot distinguish differences between bond types.

Similar results to the above have been seen for other metal complexes, for example $29 \text{ e } \text{\AA}^{-5}$ has been reported of C=O bonds.³³ The charge density studies of small peptide molecules^{34,35} are also relevant here. The ranges of $L_c(\rho)$ reported are given now, with again results from the present study in parentheses and from a theoretical calculation in square brackets: O–C bonds 9.8 to 38.5 (38) [$—$] $\text{e } \text{\AA}^{-5}$, O=C bonds 15.8 to 31.9 (34) [-4.7] $\text{e } \text{\AA}^{-5}$, N–C(H₂) bonds 5.6 to 14.4 (17) [19.4] $\text{e } \text{\AA}^{-5}$, N–C(O) bonds 17.2 to 27.7 (14) [15.0] $\text{e } \text{\AA}^{-5}$, and C–C bonds 11.1 to 14.4 (16) [20.5] $\text{e } \text{\AA}^{-5}$.

Conclusions

The agreement between the valence orbital populations and between the topological features of the bonding electron distribution for the two molecules of Cu(glygly)(OH)₂ is encouraging, and confirms ideas about their reproducibility when derived from charge density studies.

The estimation of atomic charges by any method is not of predictive chemical value but those conforming best with chemical expectations are based on the AIM and the valence orbital population approaches. The valence orbital populations also mostly conform quite well on an individual basis with simple chemical bonding pictures. However, they are rarely sufficiently accurate to differentiate between models. The exceptions are the carbonyl C atom p_π populations, which are noticeably lower than the accompanying $(sp^2)_\sigma$ values. The overall charges on water molecules are more consistent, as each method yields a lower charge for those bound to the copper ion than for the “free” O6 based molecule. However, no distinction between the O4 and the less firmly bound O5 based water molecules can be drawn.

The values of the electron densities at Cu–O and Cu–N bcp in the topological analysis are consistent with a mixed ionic/covalent type of bonding interaction. The values at the bcp between oxygen, nitrogen and carbon atoms are quite similar to those found in small peptide molecules, and little influence of the copper atom on these bonds is evident.

The values of $L_c(\rho)$ at the bcp reinforce those conclusions about bonding between copper and oxygen and nitrogen and between pairs of the three light atoms. On account of the sensitivity of the Laplacian to the detail of the electron density, the scatter of the results is greater. The disagreement between experiment and theory for the value of $L_c(\rho)$ at the C=O bcp,³⁵ ≈ 30 versus $-4.7 \text{ e } \text{\AA}^{-5}$, is confirmed.

Acknowledgements

The authors are grateful to the Australian Research Council for financial support and to one of the referees for helpful suggestions.

References

- 1 A. R. Manyak, C. B. Murphy and A. E. Martell, *Arch. Biochem. Biophys.*, 1955, **59**, 373.
- 2 B. Strandberg, I. Lindquist and R. Rosenstein, *Z. Kristallogr.*, 1961, **116**, 266.
- 3 T. J. Kistenmacher and D. J. Szalda, *Acta Crystallogr., Sect. B*, 1975, **31**, 1659.
- 4 F. K. Larsen, *Acta Crystallogr., Sect. B*, 1995, **51**, 468.
- 5 V. A. Streltsov and V. E. Zavodnik, *Sov. Phys. Crystallogr. (Engl. Transl.)*, 1989, **34**, 824.
- 6 (a) S. R. Hall, D. J. du Boulay and R. Olthof-Hazekamp, ed., XTAL 3.7 System of Crystallographic Programs, University of Western Australia, 2000; (b) T. Koritsanzky, S. Howard, P. R. Mallinson, Z. Su, T. Richter and N. K. Hansen, *XD Program Manual*, Institute for Crystallography, Free University of Berlin, 1999.
- 7 P. Becker and P. Coppens, *Acta Crystallogr., Sect. A*, 1974, **30**, 129.
- 8 G. M. Sheldrick, SHELXL97, Program for the refinement of Crystal Structures, University of Göttingen, Germany, 1997.
- 9 *International Tables for Crystallography*, Kluwer, London, 1992, vol. C, Tables 4.2.6.8 and 6.1.1.4.
- 10 E. Clementi and C. Roetti, *At. Data, Nucl. Data Tables*, 1974, **14**, 177.
- 11 R. F. Stewart, E. R. Davidson and K. T. Simpson, *J. Chem. Phys.*, 1965, **42**, 3175.
- 12 B. N. Figgis, P. A. Reynolds and S. Wright, *J. Am. Chem. Soc.*, 1983, **105**, 434.
- 13 B. N. Figgis, A. N. Sobolev, D. M. Young, A. J. Schultz and P. A. Reynolds, *J. Am. Chem. Soc.*, 1998, **120**, 8715.
- 14 Y. Le Page and E. J. Gabe, *Acta Crystallogr., Sect. A*, 1979, **35**, 73.
- 15 R. F. W. Bader, *Atoms in Molecules; a Quantum Theory*, Oxford University Press, 1990.
- 16 A. Volkov, C. Gatti, Y. Abramov and P. Coppens, *Acta Crystallogr., Sect. A*, 2000, **56**, 252.

- 17 M. J. Frisch, G. W. Trucks, H. B. Schlegel, G. E. Scuseria, M. A. Robb, J. R. Cheeseman, V. G. Zakrzewski, J. A. Montgomery, Jr., R. E. Stratmann, J. C. Burant, S. Dapprich, J. M. Millam, A. D. Daniels, K. N. Kudin, M. C. Strain, O. B. Farkas, J. Tomasi, V. Barone, M. Cossi, R. Cammi, B. Mennucci, C. Pomelli, C. Adamo, S. Clifford, J. Ochterski, G. A. Petersson, P. Y. Ayala, Q. Cui, K. Morokuma, D. K. Malick, A. D. Rabuck, K. Raghavachari, J. B. Foresman, J. Cioslowski, J. V. Ortiz, A. G. Baboul, B. B. Stefanov, G. Liu, A. Liashenko, P. Piskorz, I. Komaromi, R. Gomperts, R. L. Martin, D. J. Fox, T. Keith, M. A. Al-Laham, C. Y. Peng, A. Nanayakkara, C. Gonzalez, M. Challacombe, P. M. W. Gill, B. Johnson, W. Chen, M. W. Wong, J. L. Andres, C. Gonzalez, M. Head-Gordon, E. S. Replogle and J. A. Pople, Gaussian 98, Revision A.7, Gaussian, Inc., Pittsburgh, PA, 1998.
- 18 P. L. A. Popelier with a contribution by R. G. A. Bone, MORPHY 98, UMIST, Manchester, England, 1998.
- 19 D. L. Kepert, *Inorganic Stereochemistry*, Springer-Verlag, Berlin, 1982, pp. 65–69.
- 20 F. L. Hirshfeld, *Theor. Chim. Acta*, 1977, **44**, 129.
- 21 B. N. Figgis, E. S. Kucharski, J. M. Raynes and P. A. Reynolds, *J. Chem. Soc., Dalton Trans.*, 1990, 3597.
- 22 B. N. Figgis, L. Kohr, E. S. Kucharski and P. A. Reynolds, *Acta Crystallogr., Sect. B*, 1992, **48**, 144.
- 23 B. N. Figgis, P. A. Reynolds and A. N. Sobolev, *J. Chem. Soc., Dalton Trans.*, 1994, 1429.
- 24 E. N. Maslen and M. A. Spackman, *Aust. J. Phys.*, 1985, **38**, 273.
- 25 C. Flensburg and D. Madsen, *Acta Crystallogr., Sect. A*, 2000, **56**, 24.
- 26 D. J. Grimwood and D. Jayatilaka, *Acta Crystallogr., Sect. A*, 2001, **57**, 87.
- 27 M. A. Spackman, *Chem. Rev.*, 1992, **92**, 1769.
- 28 I. Bytheway, G. S. Chandler, B. N. Figgis, D. J. Grimwood and D. Jayatilaka, *Acta Crystallogr., Sect. A*, submitted.
- 29 I. Bytheway, D. J. Grimwood and D. Jayatilaka, *Acta Crystallogr., Sect. A*, 2001, submitted.
- 30 R. J. Gillespie, I. Bytheway and E. A. Robinson, *Inorg. Chem.*, 1998, **37**, 2811.
- 31 B. B. Iversen, F. K. Larsen, B. N. Figgis and P. A. Reynolds, *J. Chem. Soc., Dalton Trans.*, 1997, 2227.
- 32 P. Macchi, D. M. Proserpio and A. Sironi, *J. Am. Chem. Soc.*, 1998, **120**, 13429.
- 33 P. Macchi, D. M. Proserpio and A. Sironi, *J. Am. Chem. Soc.*, 1998, **120**, 1447.
- 34 F. Benabicha, V. Pichon-Pesme, C. Jelsch, C. Lecomte and A. Khmou, *Acta Crystallogr., Sect. B*, 2000, **56**, 155.
- 35 V. Pichon-Pesme, H. Lachekar, M. Souhassou and C. Lecomte, *Acta Crystallogr., Sect. B*, 2000, **56**, 728.